

Doubly Thiazole Orange-Labeled DNA for Live Cell RNA Imaging

Takeshi Kubota, Shuji Ikeda, and Akimitsu Okamoto*

Advanced Science Institute, RIKEN (The Institute of Physical and Chemical Research), Wako 351-0198

Received August 8, 2008; E-mail: aki-okamoto@riken.jp

A hybridization-sensitive, quencher-free fluorescent probe for RNA detection has been designed using the concept of fluorescence quenching caused by the intramolecular excitonic interaction of fluorescence dyes. We synthesized a doubly thiazole orange-labeled nucleoside showing high fluorescence intensity for a hybrid with the target RNA and effective quenching for the single-stranded state. The probe was applied to living HeLa cells using microinjection to visualize intracellular mRNA localization. Immediately after injection of the probe into the cell, fluorescence from the probe hybridizing with the target RNA was observed. This fluorescence rapidly decreased upon addition of a competitor DNA. This probe realized a large, rapid, and reversible change in fluorescence intensity in sensitive response to the amount of target RNA, and facilitated spatiotemporal monitoring of the behavior of intracellular RNA.

Many fluorescent nucleic acid probes have been designed for RNA detection.[1–9] Conventional fluorescent nucleic acid probes always emit fluorescence when excitation light is shone on probe-containing RNA samples. Therefore, probes that do not take part in labeling of the target RNA have to be completely removed from the sample through several troublesome washing processes to remove the background fluorescence. To effectively monitor RNA in a living cell, hybridization sensitivity of the fluorescent emission of probes is essential to avoid background fluorescence or the washing process. The point of the probe design is how we quench the fluorescence of the probe in the nonhybridization state. For this purpose, intra/intermolecular energy transfer between a fluorescent dye and a quencher and/or the formation of higher-order structures of probes have been required,[10–14] and such complicated structural demands have often induced malfunctions of probes in endogenous RNA detection. The novel photochemical design of a structurally simpler, quencher-free hybridization-sensitive probe will achieve a more sensitive response to the change in amount and distribution of the target RNA in a living cell. Here we present efficient RNA detection using a hybridization-sensitive fluorescent DNA probe controlled by an excitonic interaction of tethered dyes. This fluorescent probe showed efficient turning on/off of fluorescence depending on hybridization with the target RNA, and this unique function was applicable to spatiotemporal mRNA imaging in living cells.

Results and Discussion

Function of the Probe. We focused on the photophysical behavior of a fluorescent dye, thiazole orange (=1-methyl 4-[(3-methyl-2(3*H*)-benzothiazolylidene)methyl]quinolinium *p*-tosylate). This dye emits strong fluorescence in a DNA binding state, whereas the fluorescence of the free dye is very weak.[15,16] Much research on linking such a thiazole orange dye to an artificial DNA molecule or DNA analog and its application to gene analysis has already been reported.[17–25] Indeed, these probes show strong fluorescence, but the quenching efficiency in the single-stranded state is often low. High background fluorescence is a serious weak point of thiazole orange-labeled DNA as a probe for gene analysis. Thiazole orange dye is also known to show little emission by excitonic interaction when dyes arrange in parallel.[26–33] The design of probes showing an excitonic interaction by the coupling of two thiazole orange dyes is expected to produce a highly sensitive probe system. On the basis of this concept, we have designed a doubly thiazole orange-labeled nucleoside to achieve high fluorescence intensity for a hybrid with the target DNA and effective quenching for a single-stranded state of the probe (Figure 1a).[34] An excitonic interaction was produced by the formation of an aggregate between dyes, and as a result, emission from the probe before hybridization was suppressed. Dissociation of aggregates by hybridization with the cDNA resulted in strong emission from the hybrid. If the aggregation/dissociation of dyes can also be controlled by hybridization with RNA, this feature would be valuable for the design of a quencher-free RNA detection probe.

We synthesized fluorescent nucleic acids with a bis(thiazole orange)-labeled uridine as a conceptually new RNA detection probe. A synthetic nucleoside with two amino linkers was prepared from a uridine derivative with an acrylate group at C5, which was then incorporated into DNA strands through a conventional phosphoramidite method by using a DNA autosynthesizer.[34] A doubly fluorescence-labeled probe was obtained by mixing the synthesized diamino-DNA with a carboxy-activated thiazole orange derivative (Figure 1b). ODN1 was designed to recognize an RNA polyA tail. Nontargeting strands ODN2 and ODN3 were also prepared. These fluorescent DNA strands greatly changed their fluorescence intensities on hybridization with the complementary RNA strands. For example, ODN1 displayed negligible fluorescence in the single-strand state in pseudo-intracellular buffer solution (5 mM sodium chloride, 120 mM potassium chloride, 25 mM HEPES, pH 7.2 (1 M = 1 mol dm^{-3})). On the other hand, after mixing with one equivalent of an A 13-mer (A_{13}) RNA, the clear yellow-green fluorescence of ODN1 was

Published on the web January 14, 2009; doi:10.1246/bcsj.82.110

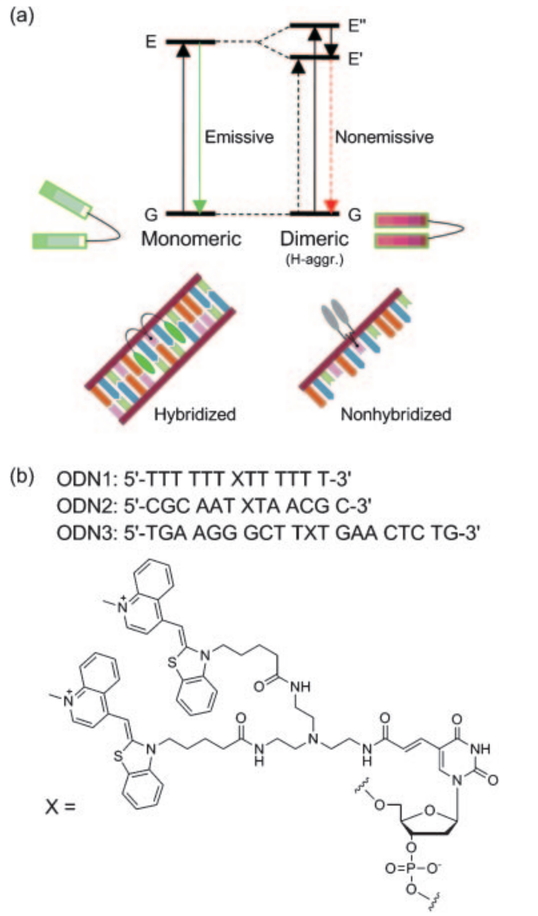

Figure 1. Newly designed hybridization probe controlled by exciton coupling between thiazole orange dyes. (a) Fluorescent emission control by the excitonic interaction between thiazole orange dyes. (b) Synthesized DNA sequences.

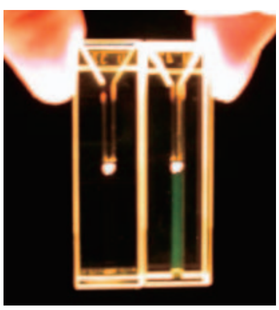

Figure 2. Fluorescence emission in cuvettes. A solution containing 1 μM ODN1 in the presence (right) or absence (left) of one equivalent of A_{13} RNA in 5 mM NaCl, 120 mM KCl, and 25 mM HEPES (pH 7.2)–KOH was irradiated with a 150-W halogen lamp.

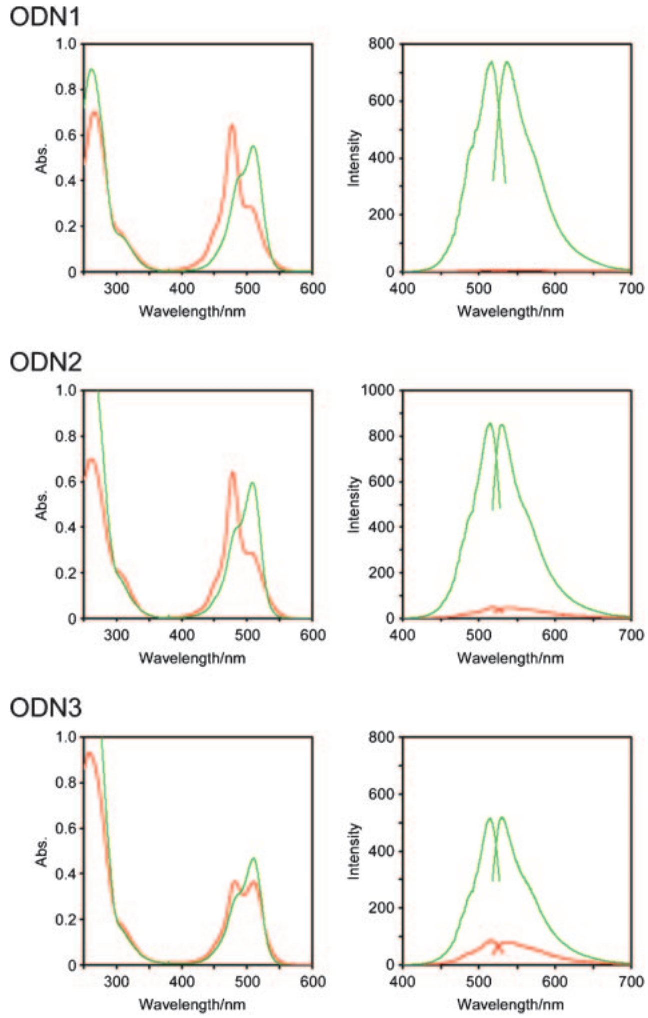

Figure 3. Absorption, excitation, and fluorescence spectra. Absorption spectra (5 μM) are shown in the left panels and excitation and fluorescence spectra (2 μM) are shown in the right panels. These spectra were measured in 5 mM NaCl, 120 mM KCl, and 25 mM HEPES (pH 7.2)–KOH at 25 °C. Red, single strand (ss); green, hybrid with one equivalent of the complementary RNA (ds). Excitation spectra of ODNs for ss and ds were measured for emission at 538 and 536 nm (ODN1), at 534 and 530 nm (ODN2), and at 536 and 530 nm (ODN3), respectively. The samples, ss and ds, for emission spectra were excited at 516 nm (ODN1), at 519 and 514 nm (ODN2), at 516 and 515 nm (ODN3), respectively.

observed under white light illumination (Figure 2). The reason for the hybridization-sensitive change in the fluorescence intensity can be explained by the shift in the absorption maximum. The absorption spectrum before hybridization showed a strong band at 477 nm, whereas this strong band after hybridization was shifted to 510 nm (Figure 3). The shift in the absorption band indicates that the switching of excitonic interaction between tethered thiazole orange dyes worked effectively before/after hybridization with the RNA strand. The absorption at a shorter wavelength before hybridization is caused by excitation to the upper energy level of the excited state of the dyes; which is split into two energy levels, this splitting being due to H-aggregation of the dyes.[35] The excitation rapidly deactivates to the lower excitonic state, from which emission is theoretically forbidden. When hybridization with the target RNA induces dissociation of the dye aggregate, each dye becomes bright. A large enhancement of the intensity on hybridization with the RNA strand was observed in both excitation and fluorescence spectra. The fluorescence ratio at

Table 1. Photophysical Properties of ODN1–3[a)]

ODNs[b)]		λ_{max}/nm	ε/cm^{-1} M^{-1}	Φ_f	λ_{em}/nm[c)]	I_{ss}[d)]	I_{ds}/I_{ss}	T_m/°C[e)]
ODN1	(ss)	477	128780					
		503	56820	0.01	543 (516)	6.0		
	(ds)	510	110220	0.51	537 (516)		116	58 (32)
ODN2	(ss)	478	128220					
		504	57700	0.04	537 (519)	48.3		
	(ds)	509	119060	0.37	530 (514)		20	54 (46)
ODN3	(ss)	482	73380					
		510	72840	0.09	536 (516)	80.5		
	(ds)	510	93700	0.25	531 (515)		7	72 (66)

a) Measured in 5 mM NaCl, 120 mM KCl, 25 mM HEPES (pH 7.2)–KOH. b) ss = single-stranded state, ds = hybrid with the complementary RNA. c) Excitation wavelength is in parentheses. d) Maximum of fluorescent intensity for the single-stranded state (2 µM). e) The T_m values for the hybrids of the natural DNA and the complementary RNA are in parentheses.

Table 2. Fluorescence Ratio of ODN1 before and after Mixing with Different RNA Sequences[a)]

Hybridized RNA	Ratio
—	1.0 (the standard)
5′-UUUUUUUUUUUUU-3′	1.0
5′-GCGUUAAAUUGCG-3′	1.0
5′-CAGAGUUCAAAAGCCCUUCA-3′	1.2
5′-AAAAAAAAAAAAA-3′	116
PolyA	97

a) Measured in 5 mM NaCl, 120 mM KCl, 25 mM HEPES (pH 7.2)–KOH. $\lambda_{ex} = 516$ nm, $\lambda_{em} = 537$ nm.

537 nm was 116 (Table 1). This significant change in fluorescence intensity occurred selectively for the target RNA sequence; thus, the fluorescence change was very small upon addition of other irrelevant RNAs (<1.2, Table 2). The photophysical behavior of ODN2 and ODN3 before/after hybridization with the corresponding complementary RNA also changed in a similar manner to that of ODN1, as seen in Figure 3. We also measured the fluorescence of a mixed sequence ODN2 hybridized with several RNA strands containing mismatched nucleotides. The hybridization with a mismatched RNA showed higher fluorescence intensity than that of the single-stranded ODN2, but lower compared with that of the hybridization with full-matched RNA (Figure 4). The data in Figure 4 is similar to the fluorescence behavior observed for hybrids with mismatched DNA strands reported previously.[36] We also investigated the fluorescence intensity of ODN2 in sodium phosphate buffer with pH 5–9. The fluorescence intensity of thiazole orange dye is almost insensitive to the pH changes,[37] and this probe was also tolerant toward various pHs. The fluorescence intensity was almost constant (±10%), regardless of the range of pH. The ratio of the fluorescence intensities for double- and single-stranded states (I_{ds}/I_{ss}) was 15–21 under the conditions used. When the DNA probe had only one thiazole orange dye, the degree of fluorescence quenching in the single-strand state became smaller (Figure 5). Observation of no shift of the absorption band to shorter wavelength in the single-strand state suggests that ODN2(X′) did not form an H-aggregate. Because the exciton coupling effect does not work when an H-aggregate is

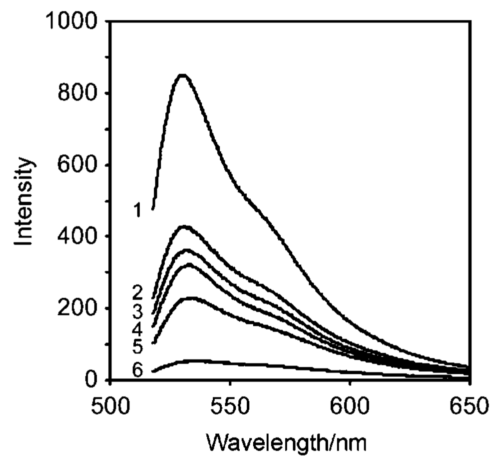

Figure 4. Fluorescence spectra of mismatched duplexes. The spectra of mismatched duplexes (2 µM) were measured in 5 mM NaCl, 120 mM KCl, and 25 mM HEPES (pH 7.2)–KOH at 25 °C. DNA samples were excited at 514 nm. The RNA strands hybridized with ODN2 were 1: 5′-GCGUUAAAUUGCG-3′ (matched); 2: 5′-GCGUUAA-CUUGCG-3′; 3: 5′-GCGUUAGAUUGCG-3′; 4: 5′-GCG-UUACAUUGCG-3′; 5: 5′-GCGUUAUAUUGCG-3′; 6: 5′-GCGUUCACUUGCG-3′.

not formed, the fluorescence quenching in the single-strand state is smaller than that of ODN2 in Figure 3, although there is still the structural control of fluorescence due to the constrictive DNA environment.

The fluorescence intensity is very sensitive to the existence of the complementary RNA strand. ODN1 formed a highly stable hybrid with A_{13} RNA, the melting temperature (T_m) of the hybrid being 58 °C, which is much higher than that of the corresponding unmodified T_{13} DNA/A_{13} RNA hybrid (32 °C). Binding of two cationic dyes to the hybrid resulted in the thermally stabilization of the labeled hybrid. Therefore, the formation of the hybrid is rapid after mixing ODN1 and A_{13} RNA. The fluorescence increased immediately after mixing and reached over 90% in 30 s (Figure 6). The fluorescence intensity of ODN1 exhibited a linear relationship with the amount of ODN1 at a constant concentration of A_{13} RNA (Figure 7). The fluorescence intensity of an ODN1-containing solution increas-

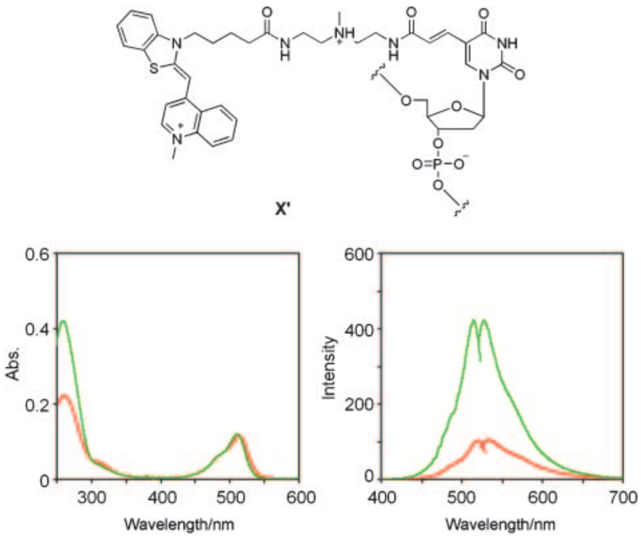

Figure 5. Absorption, excitation, and fluorescent spectra of singly dye-labeled DNA. A singly dye-labeled DNA ODN2(X′), 5′-CGCAATX′TAACGC-3′, was prepared and the absorption and fluorescent spectra of its single-strand state and the hybrid with the complementary RNA 5′-GCGUUAAAUUGCG-3′ were measured. Absorption spectra (5 µM) are shown in the left panels and excitation and fluorescent spectra (2 µM) are shown in the right panels. These spectra were measured in 5 mM NaCl, 120 mM KCl, and 25 mM HEPES (pH 7.2)–KOH at 25 °C. Red, single strand (ss); green, hybrid with one equivalent of the complementary RNA (ds). Excitation spectra for ss and ds were measured for emission at 534 and 528 nm, respectively. Samples, ss and ds, for emission spectra were excited at 519 and 515 nm, respectively.

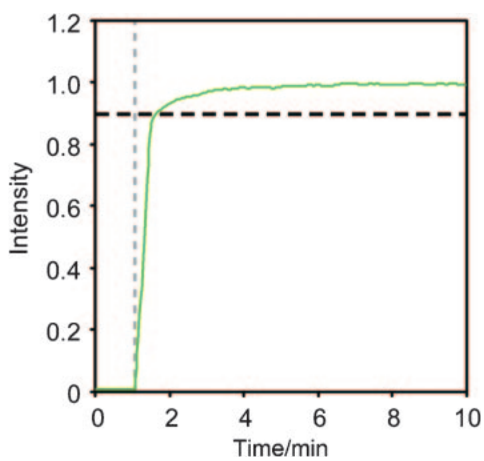

Figure 6. Addition of A_{13} RNA to a solution of ODN1. ODN1, 3.0 µM; A_{13} RNA, 3.2 µM. $\lambda_{ex} = 510$ nm, $\lambda_{em} = 540$ nm. The gray dashed line shows the injection point of A_{13} RNA at 1 min. The black dashed line shows 90% of the fluorescence intensity (0.9). The fluorescence intensity at 10 min after incubation is normalized to 1.0.

ed in proportion to the amount of added A_{13} RNA and almost reached a plateau when the ODN1:A_{13} RNA ratio became 1:1. This change in the fluorescence intensity of the probe showing sensitivity to the amount of target RNA may be advantageous for tracing intracellular RNA fluctuations.

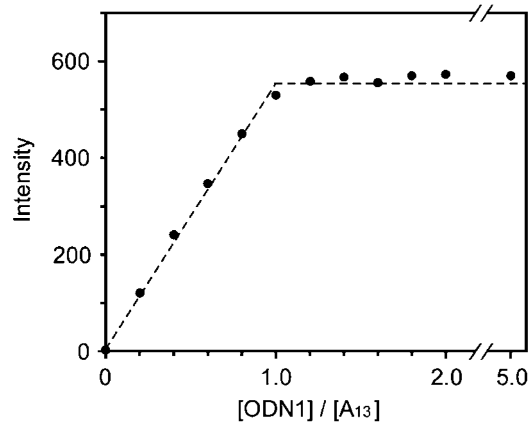

Figure 7. A linear relationship between the amount of ODN1 and the fluorescence intensity. The fluorescence intensity of ODN1 was measured in 5 mM NaCl, 120 mM KCl, and 25 mM HEPES (pH 7.2)–KOH containing 0.1 µM A_{13} RNA and 0, 0.02, 0.04, 0.06, 0.08, 0.1, 0.12, 0.14, 0.16, 0.18, 0.20, and 0.50 µM ODN1 at 25 °C. $\lambda_{ex} = 516$ nm (bandwidth, 1.5 nm); $\lambda_{em} = 537$ nm (bandwidth, 3.0 nm).

Live Cell Imaging. We next applied the ODN1 strand to living HeLa cells using manipulator-assisted microinjection to visualize intracellular mRNA localization. Immediately after injection of the ODN1 to the cytoplasm area, fluorescence was observed from both the nucleus and cytoplasm of the cell on excitation at 488 nm (Figure 8), which was identified as emission from ODN1 by the fluorescence spectrum produced from the data obtained from a multichannel spectrum detector (Figure 9). The distribution pattern of fluorescence was similar to the results reported previously on mRNA distribution observed for fixed cells.[3,38] The very strong fluorescence from the nucleus originates from binding of ODN1 with RNA, not with DNA. ODN1 emits little fluorescence in the presence of duplex DNA (Figure 10). Although nontarget probes (ODN2 and ODN3) were also applied to living cells under the condition that the gain of the detector and excitation power were both fixed throughout these experiments to eliminate disturbance, the images showed quite different appearances from that obtained with ODN1. The cells that were injected with either ODN2 or ODN3 exhibited negligible fluorescence emission. The observed emission behavior suggests that ODN1 stained the polyA tail of endogenous RNA, and these probes did not exhibit nonspecific emission originating from binding to other cell components.

The fluorescence intensity of the probe is variable because the amount of hybridizable RNA always changes with time. The fluorescence from a mixture of ODN1 and polyA RNA rapidly decreased by competitive hybridization of a T 70-mer (T_{70}) DNA (Figure 11), suggesting that ODN1 was replaced by a T_{70} DNA, which forms a more stable duplex with polyA RNA ($T_m = 61$ °C); thus ODN1 lost its brightness. Such quenching with T_{70} was also observed for ODN1 hybridizing with mRNA in a living cell. The T_{70} strand was injected into the cell that had emitted fluorescence resulting from injection of ODN1 (Figure 12). The fluorescence intensity of the T_{70}-

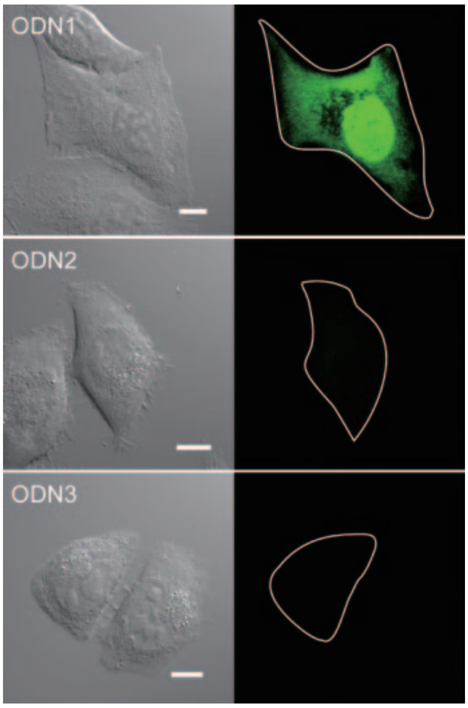

Figure 8. Differential interference contrast (DIC) and fluorescence images of probe-injected HeLa cells. The sample was excited at 488 nm, and the fluorescence was collected through a 505–550 nm band-pass filter. White lines in the fluorescent images show the edge of the probe-injected cells. Bar, 10 µm.

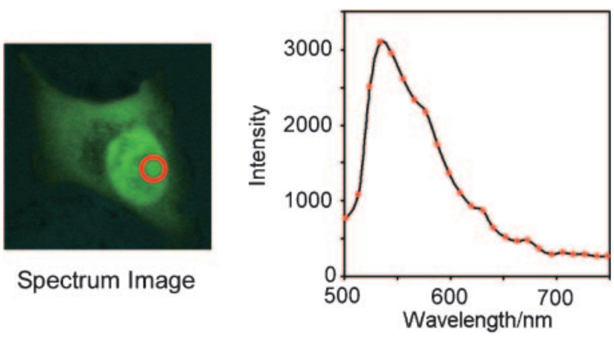

Figure 9. Fluorescence spectrum image. The image of ODN1 was acquired from the cell of Figure 8 using a multichannel detector. The fluorescence intensities of the area shown by a red circle were collected at 24 different wavelengths.

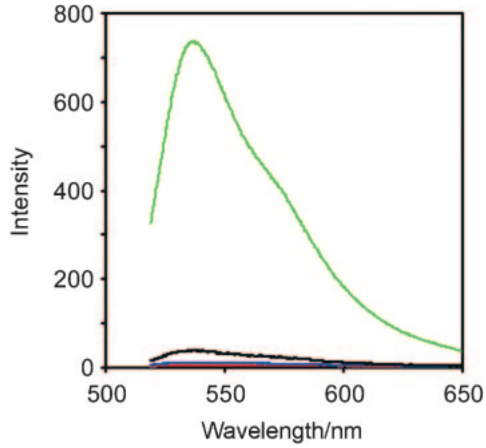

Figure 10. Low fluorescence intensity of ODN1 in the presence of duplex DNA. The spectra of mixtures of DNA duplexes and ODN1 were measured in 5 mM NaCl, 120 mM KCl, and 25 mM HEPES (pH 7.2)–KOH at 25 °C. The samples were excited at 516 nm. Red, single-stranded ODN1 (2 µM); green, hybrid with one equivalent of the complementary RNA (2 µM); black, a mixture containing a poly(dA)/poly(dT) DNA duplex (10 µg); blue, a mixture containing salmon sperm DNA (10 µg).

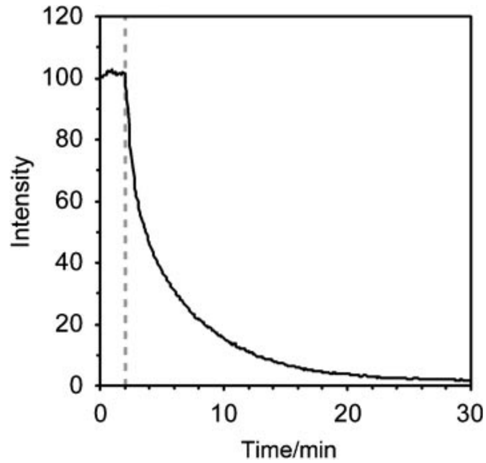

Figure 11. Time-course of fluorescence intensity before and after the addition of T_{70} DNA in vitro. T_{70} DNA (500 pmol) was added to a solution of ODN1 (200 pmol) and polyA RNA (6.0 µg). Fluorescence was measured every 5 s for 30 min in a pseudo-intracellular buffer (1600 µL, 5 mM NaCl, 120 mM KCl, 25 mM HEPES (pH 7.2)–KOH) at 37 °C. Gray dashed line at 2 min indicates the time of the T_{70} addition. $\lambda_{ex} = 488$ nm (bandwidth, 1.5 nm); $\lambda_{em} = 537$ nm (bandwidth, 3.0 nm).

injected cell decreased to 50% within 50 s of injection, whereas the decrease in the fluorescence intensity of the cell where T_{70} had not been injected was less than 2%. The decrease in the fluorescence intensity of the control cell is probably due to the bleaching of dye, dissociation from the target RNA, or degradation of ODN1 and RNA by intracellular enzymes. In fact, the doubly thiazole orange-labeled DNA probes were digested with a powerful exonuclease, snake venom phosphodiesterase, as fast as the degradation of natural single-stranded DNA, although the digestion of the probe hybridized with the target RNA was strongly suppressed. In addition, when an endonuclease RNase H was added to a mixture of ODN1 and A_{13} RNA, the fluorescence decreased gradually, showing the RNA degradation of probe–RNA hybrids.

These marked changes in the photophysical behavior of doubly thiazole orange-labeled DNA probes that are dependent on RNA strands play a key role in spatiotemporal imaging of the target RNA expressed in a living cell. We also tested an imaging of the RNA expressing from the vector encoding a *Discosoma* sp. red fluorescent protein DsRed2 (pDsRed2-Mito).[39] A doubly thiazole orange-labeled DNA ODN4 was

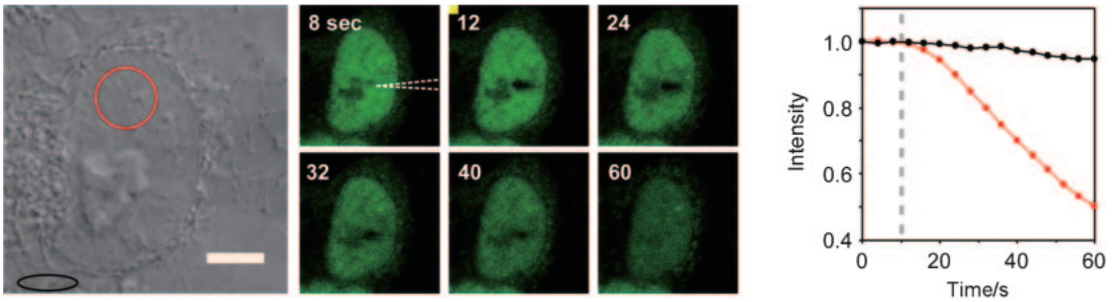

Figure 12. Decrease in the fluorescence from probe-injected HeLa cells after injection of T_{70} DNA. The sample was excited at 488 nm, and the fluorescence was collected through a 505–550 nm band-pass filter. Time-lapse images (left) and time-dependent change in fluorescence intensity (right). The circles drawn in the DIC image indicate the measured area, and the color of the circles corresponds to the color of the plots in the right hand panel (red, nucleus of the target ODN1-injected cell; black, cytoplasm of another ODN1-injected cell). The white dashed line in the fluorescence image indicates the point of injection. The gray dashed line in the time-course figure indicates the time of the T_{70} DNA injection (500 µM). Fluorescence was measured every 4 s. Bar, 5 µm.

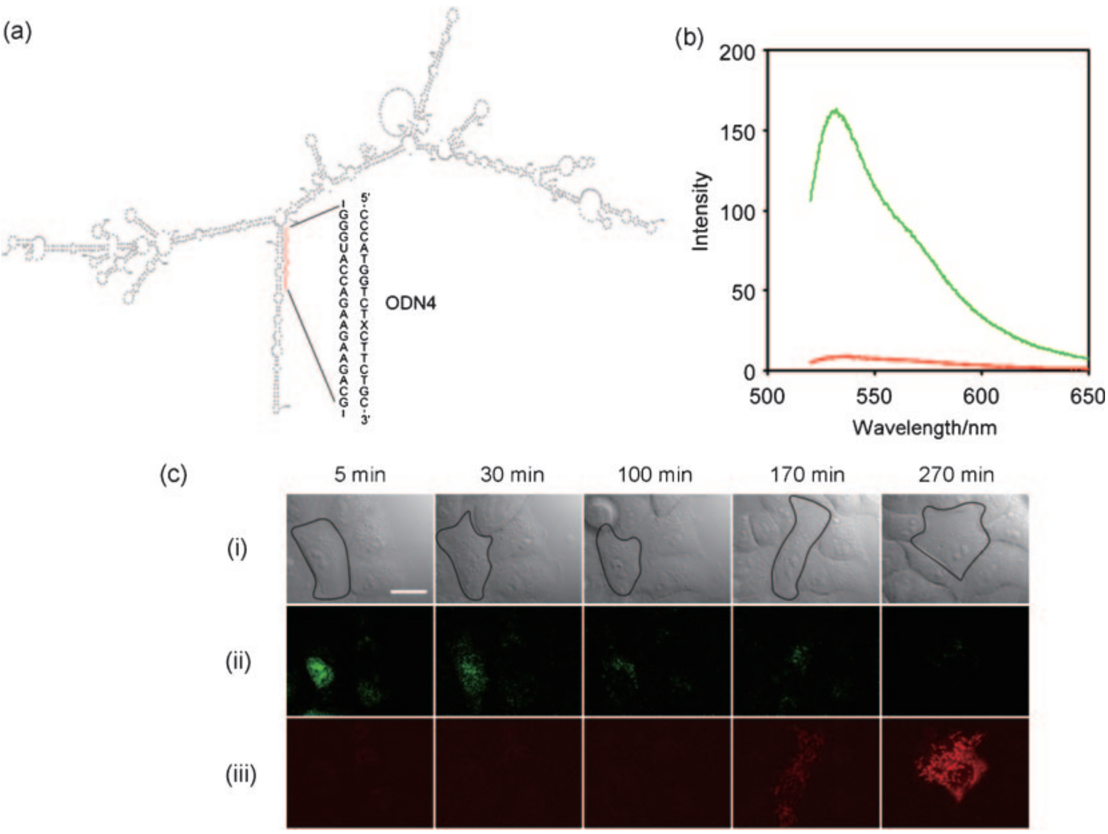

Figure 13. Spatiotemporal DsRed2-Mito mRNA imaging in a living cell. (a) Plausible secondary structure of DsRed2-Mito RNA and the sequence of RNA detection probe ODN4. (b) Fluorescence emission spectra of ODN4 in vitro. These spectra (0.5 µM) were measured in 5 mM NaCl, 120 mM KCl, and 25 mM HEPES (pH 7.2)–KOH at 25 °C. Red, single strand (ss); green, hybrid with one equivalent of the corresponding complementary RNA (ds). $\lambda_{ex} = 514$ nm (bandwidth, 1.5 nm). (c) Expression of DsRed2-Mito mRNA and protein. Time-lapse images were taken at 5, 30, 100, 170, and 270 min after injection of ODN4 (10 µM) and pDsRed2-Mito (500 ng µg^{-1}) into a HeLa cell. (i) DIC image. Bar, 20 µm. Black lines in the fluorescence images show the edge of the probe-injected living cell. (ii) Fluorescence from ODN4. The sample was excited at 514 nm, and the fluorescence was collected through a 520–555 nm band-pass filter. (iii) Fluorescence from DsRed2 fluorescent protein. The sample was excited at 543 nm and the fluorescence was collected through a 560 nm long-pass filter.

synthesized as a probe, capable of binding to a mismatch-rich stem region in the plausible secondary structure[40] of DsRed2-Mito RNA (Figure 13a). The fluorescence of ODN4 hybridized with the complementary RNA strand was strong and completely distinguishable from the significantly suppressed fluorescence of single-stranded ODN4 ($I_{ds}/I_{ss} = 20$) (Figure 13b). A mixture of ODN4 and pDsRed2-Mito plasmid vector was injected into a HeLa cell (The mixture showed no fluorescence.), and then the spatiotemporal change in fluorescence emission in the cell was observed. Fluorescence emission from

ODN4 was mainly observed in the nucleus 5 min after injection (Figure 13c), and then the green fluorescence extended to the entire cell (30 min). Red fluorescence has appeared while green fluorescence weakens gradually (100–270 min). The spatiotemporal change in fluorescence from the cell suggests that (i) the information of the vector transcribed to RNA in the nucleus (5 min), (ii) the RNA moved to the cytoplasm (30 min), (iii) the information of the RNA was translated to DsRed2 protein monomer, (iv) the ODN4–RNA hybrid was decomposed gradually (100–270 min), and (v) the DsRed2 protein formed the tetrameric structure to emit red fluorescence (170–270 min). When the plasmid vector was not injected, fluorescence from the cell by the injection of ODN4 was not observed at all. We detected the mRNA taking part in protein expression using the green fluorescence of the doubly thiazole orange-labeled DNA probe.

Conclusion

In conclusion, we have designed a hybridization-sensitive, quencher-free fluorescent probe for RNA detection using the concept of fluorescence quenching caused by excitonic interaction. This probe realized a large, rapid, and reversible change in fluorescence intensity in sensitive response to the amount of target RNA, and facilitated effective monitoring of the behavior of intracellular RNA. Although there still remain further aspects to be examined toward an easier-to-use intracellular RNA analysis, such as molecular design for resistance to nuclease digestion and further improvement of transfection method, we anticipate that this new concept of the hybridization-sensitive probe supported by the photochemical basis will be the starting point of the development of a practical assay for detection of RNAs in living cells and monitoring of their spatiotemporal characteristics.

Experimental

Probe Synthesis. DNA oligomers were synthesized by a conventional phosphoramidite method using an Applied Biosystems 392 DNA/RNA synthesizer. Commercially available phosphoramidites were used for dA, dG, dC, and dT. The diamino-modified nucleoside phosphoramidite, which was modified with thiazole orange dyes, was synthesized according to our previous report.[34] The synthesized DNA oligomer was cleaved from the support with 28% aqueous ammonia and deprotected at 55 °C for 4 h and then at 25 °C for 16 h. After removal of ammonia from the solution under reduced pressure, the DNA was purified by reversed-phase HPLC on a 5-ODS-H column (10 mm × 150 mm, elution with a solvent mixture of 0.1 M triethylamine acetate (TEAA), pH 7.0, linear gradient over 30 min from 5% to 30% acetonitrile at a flow rate of 3.0 mL min^{-1}). For determination of the concentration of each DNA, the purified DNA was fully digested with calf intestine alkaline phosphatase (50 U mL^{-1}), snake venom phosphodiesterase (0.15 U mL^{-1}), and P1 nuclease (50 U mL^{-1}) at 25 °C for 16 h. Digested solutions were analyzed by HPLC on a CHEMCOBOND 5-ODS-H column (4.6 mm × 150 mm), elution with a solvent mixture of 0.1 M TEAA, pH 7.0, and flow rate of 1.0 mL min^{-1}. The concentration was determined by comparing peak areas with a standard solution containing dA, dC, dG, and dT at concentrations of 0.1 mM.

A solution of *N*-{4-[2-(1-methylquinolinio-4-yl)methylidene-3-benzothiazolyl]butylcarbonyloxy}succinimide[34] (50 equiv to an active amino group of DNA) in DMF was added to a solution of deprotected DNA in 100 mM sodium carbonate buffer (pH 9.0), and incubated at 25 °C for 16 h. The reaction mixture was diluted with ethanol. After centrifuging at 4 °C for 20 min, the supernatant was removed. The residue was dissolved with a small amount of water and then the solution was passed through a 0.45 µm filter. The product was purified by reversed-phase HPLC on a 5-ODS-H column (10 mm × 150 mm, elution with a solvent mixture of 0.1 M TEAA, pH 7.0, linear gradient over 30 min from 5% to 30% acetonitrile at a flow rate of 3.0 mL min^{-1}). The concentration of the fluorescent DNA was determined by the same method as described in the DNA synthesis. The fluorescent DNA was identified by MALDI-TOF mass spectrometry. ODN1, TTTTTTXTTTTTT, calcd for $C_{184}H_{227}N_{34}O_{92}P_{12}S_2$ ($[M - H]^+$) 4822.8, found 4821.4; ODN2, CGCAATXTAACGC, calcd for $C_{180}H_{217}N_{56}O_{78}P_{12}S_2$ ($[M - H]^+$) 4848.8, found 4851.4; ODN3, TGAAGGGCTTXTGAACTCTG, calcd for $C_{251}H_{305}N_{81}O_{124}P_{19}S_2$ ($[M - H]^+$) 7093.2, found 7092.3; ODN4, CCCATGGTCTXCTTCTGC, calcd for $C_{227}H_{281}N_{63}O_{115}P_{17}S_2$ ($[M - H]^+$) 6322.7, found 6324.5.

DNA and RNA. Salmon sperm DNA was purchased from Invitrogen. The DNA duplex Poly(dA)/poly(dT) was obtained from Sigma. Short RNA strands were obtained from Nippon Gene and Gene Design (Japan). The pDsRed2-Mito plasmid vector was obtained from Clontech. The secondary structure of DsRed2 mRNA was predicted with the program RNAfold (Vienna RNA package).[40]

Absorption and Fluorescence Measurements. Absorption spectra of single-strand/hybridized probes were measured using a spectrophotometer (UV2550, SHIMADZU) in pseudo-intracellular buffer solution (5 mM NaCl, 120 mM KCl, 25 mM HEPES (pH 7.2)–KOH). In the fluorescence measurements for pH effect, sodium phosphate buffers were used (pH 5, 7, and 9). Excitation and emission spectra were measured using a spectrofluorophotometer (RF-5300PC; SHIMADZU) in the buffer. Excitation spectra of ODN1 were detected at 538 and 536 nm with complementary RNA and without the RNA, respectively, the fluorescence excitation being at 516 nm in both cases. Magnesium salt was added for the RNase H experiment (5 mM $MgCl_2$). Spectra were measured at 25 °C, and time-course data were obtained at 37 °C. The excitation and emission bandwidths were 1.5 nm. The fluorescence quantum yield (Φ) was determined using 9,10-diphenylanthracene as a reference, with a known $\Phi = 0.95$ in ethanol. The quantum yield was calculated using the following equation:

$$\Phi_{(S)}/\Phi_{(R)} = [A_{(S)}/A_{(R)}] \times [(\mathrm{Abs})_{(R)}/(\mathrm{Abs})_{(S)}] \times [n_{(S)}{}^2/n_{(R)}{}^2] \quad (1)$$

Here, $\Phi_{(S)}$ and $\Phi_{(R)}$ are the fluorescence quantum yields of the sample and the reference, respectively. The terms $A_{(S)}$ and $A_{(R)}$ are the areas under the fluorescence spectra of the sample and the reference, respectively, $(\mathrm{Abs})_{(S)}$ and $(\mathrm{Abs})_{(R)}$ are the optical densities of the sample and the reference solution at the wavelength of excitation, respectively, and $n_{(S)}$ and $n_{(R)}$ are the values of the refractive index for the solvents used for the sample ($n_{(S)} = 1.333$) and the reference ($n_{(R)} = 1.383$), respectively.

Cell Culture. Dulbecco's modified Eagle's medium (DMEM) and fetal bovine serum (FBS) were purchased from GIBCO. Reagents for culturing were obtained from Sigma. HeLa cells were cultured at 37 °C in DMEM containing 10% heat-inactivated FBS, 25 U mL^{-1} penicillin, and 25 mg mL^{-1} streptomycin, under a humidified atmosphere with 5% CO_2. For experimental use, cells (passage numbers 5–9) were cultured in glass-base dishes

(Corning). Before microscope observation, the culture medium was exchanged to phenol red-free DMEM (GIBCO). Cells were maintained in the culturing condition by an incubation system (INU, Tokai Hit) during the observation.

Imaging. Images were acquired with a motorized inverted microscope (Axio Observer Z1, Zeiss) equipped with objectives (C-Apochromat 40 × water immersion NA 1.2, PlanApochromat 63 × oil immersion NA 1.4). Differential interference contrast fluorescent images were acquired with a confocal unit LSM 510 META (Zeiss) equipped with Ar and He-Ne lasers. The probes (ODN1–3) were excited at 488 nm and the fluorescence was collected with a 505–550 nm band-pass filter or a multichannel spectrum detector. The fluorescence images of ODN4 and DsRed2 were acquired sequentially (ODN4, excitation 514 nm, emission 520–555 nm band-pass filter; DsRed2, excitation 543 nm, emission 560 nm long-pass filter). Acquired images were analyzed and processed with Zeiss software (ZEN 2007, Zeiss). Microinjection was performed using a pneumatic injector (FemtoJet express, eppendorf) with glass needles (FemtoTip, eppendorf) and 3-D manipulators (Narishige). Injection of ODN1–3 was performed at 130 hPa for 0.3 s in each cell (ca. 100 fL). The injected concentrations of ODN1–3 were normalized by the fluorescent intensities in the single-stranded states (ODN1, 200 μM; ODN2, 24 μM; ODN3, 16 μM). Excitation power (percentage of the laser output, 1.05%) and the gain of the detector (854) were fixed throughout these experiments. ODN4 and pDsRed2-Mito plasmid vector (Clontech) were mixed and injected simultaneously (ODN4, 10 μM; pDsRed2-Mito, 500 ng μL^{-1}) at 160 hPa for 0.6 s. In several experiments, one extra injector was installed to inject two different solutions sequentially. Approximately 30% of the cells showed an abnormal change in cell shape as a result of the injection; those cells were not used in the experiments.

Digestion with Nucleases. ODN2 (200 pmol) was digested with snake venom phosphodiesterase (5 μU) in 10 mM Tris-HCl, 50 mM sodium chloride, 10 mM magnesium chloride, and 1 mM DTT (pH 7.9) at 37 °C. The single-stranded ODN2 was degraded completely in ten minutes. The ODN2 hybridized with the complementary RNA showed $t_{1/2} = 96$ min.

RNase H (10 U) was also added to a mixture of ODN1 and A_{13} RNA in pseudo-intracellular buffer solution (5 mM NaCl, 120 mM KCl, 25 mM HEPES (pH 7.2)–KOH) at 37 °C, and decrease in the fluorescence intensity was measured at 540 nm. RNase H, 10 U. $\lambda_{ex} = 510$ nm. The fluorescence from the ODN1–RNA hybrid decreased to 80% of the original after 17 min.

We thank Dr. Takehiro Suzuki (Biomolecular Characterization Team, RIKEN) for the MALDI-TOF mass spectrometry.

References

1 S. Paillasson, M. Van De Corput, R. W. Dirks, H. J. Tanke, M. Robert-Nicoud, X. Ronot, *Exp. Cell Res.* **1997**, *231*, 226.
2 K. Yamana, R. Iwase, S. Furutani, H. Tsuchida, H. Zako, T. Yamaoka, A. Murakami, *Nucleic Acids Res.* **1999**, *27*, 2387.
3 C. Molenaar, S. A. Marras, J. C. M. Slats, J.-C. Truffert, M. Lemaître, A. K. Raap, R. W. Dirks, H. J. Tanke, *Nucleic Acids Res.* **2001**, *29*, e89.
4 R. W. Dirks, C. Molenaar, H. J. Tanke, *Histochem. Cell Biol.* **2001**, *115*, 3.
5 J. Pernthaler, F. O. Glöckner, W. Schönhuber, R. Amann, *Methods Microbiol.* **2001**, *30*, 207.
6 G. J. Smith, T. R. Sosnick, N. F. Scherer, T. Pan, *RNA* **2005**, *11*, 234.
7 U. Asseline, *Curr. Org. Chem.* **2006**, *10*, 491.
8 A. A. Marti, S. Jockusch, N. Stevens, J. Ju, N. J. Turro, *Acc. Chem. Res.* **2007**, *40*, 402.
9 A. P. Silverman, E. T. Kool, *Adv. Clin. Chem.* **2007**, *43*, 79.
10 J. Perlette, W. Tan, *Anal. Chem.* **2001**, *73*, 5544.
11 X. Fang, Y. Mi, J. J. Li, T. Beck, S. Schuster, W. Tan, *Cell Biochem. Biophys.* **2002**, *37*, 71.
12 D. P. Bratu, B.-J. Cha, M. M. Mhlanga, F. R. Kramer, S. Tyagi, *Proc. Natl. Acad. Sci. U.S.A.* **2003**, *100*, 13308.
13 W. Tan, K. Wang, T. J. Drake, *Curr. Opin. Chem. Biol.* **2004**, *8*, 547.
14 G. Goel, A. Kumar, A. K. Puniya, W. Chen, K. Singh, *J. Appl. Microbiol.* **2005**, *99*, 435.
15 L. G. Lee, C. H. Chen, L. A. Chiu, *Cytometry, Part A* **1986**, *7*, 508.
16 J. Nygren, N. Svanvik, M. Kubista, *Biopolymers* **1998**, *46*, 39.
17 D. Hanafi-Bagby, P. A. E. Piunno, C. C. Wust, U. J. Krull, *Anal. Chim. Acta* **2000**, *411*, 19.
18 N. Svanvik, J. Nygren, G. Westman, M. Kubista, *J. Am. Chem. Soc.* **2001**, *123*, 803.
19 X. Wang, U. J. Krull, *Anal. Chim. Acta* **2002**, *470*, 57.
20 O. Köhler, D. V. Jarikote, O. Seitz, *Chem. Commun.* **2004**, 2674.
21 X. Wang, U. J. Krull, *Bioorg. Med. Chem. Lett.* **2005**, *15*, 1725.
22 D. V. Jarikote, O. Köhler, E. Socher, O. Seitz, *Eur. J. Org. Chem.* **2005**, 3187.
23 U. Asseline, M. Chassignol, Y. Aubert, V. Roig, *Org. Biomol. Chem.* **2006**, *4*, 1949.
24 R. Lartia, U. Asseline, *Chem.—Eur. J.* **2006**, *12*, 2270.
25 V. L. Marin, B. A. Armitage, *Biochemistry* **2006**, *45*, 1745.
26 W. West, S. Pearce, *J. Phys. Chem.* **1965**, *69*, 1894.
27 V. Czikklely, H. D. Forsterling, H. Kuhn, *Chem. Phys. Lett.* **1970**, *6*, 207.
28 W. J. Harrison, D. L. Mateer, G. J. T. Tiddy, *J. Phys. Chem.* **1996**, *100*, 2310.
29 R. F. Khairutdinov, N. Serpone, *J. Phys. Chem. B* **1997**, *101*, 2602.
30 S. Zeena, K. G. Thomas, *J. Am. Chem. Soc.* **2001**, *123*, 7859.
31 K. C. Hannah, B. A. Armitage, *Acc. Chem. Res.* **2004**, *37*, 845.
32 A. Fürstenberg, M. D. Julliard, T. G. Deligeorgiev, N. I. Gadjev, A. A. Vasilev, E. Vauthey, *J. Am. Chem. Soc.* **2006**, *128*, 7661.
33 U. Rösch, S. Yao, R. Wortmann, F. Würthner, *Angew. Chem., Int. Ed.* **2006**, *45*, 7026.
34 S. Ikeda, A. Okamoto, *Chem. Asian J.* **2008**, *3*, 958.
35 M. Kasha, *Radiat. Res.* **1963**, *20*, 55.
36 S. Ikeda, T. Kubota, K. Kino, A. Okamoto, *Bioconjugate Chem.* **2008**, *19*, 1719.
37 S. Ikeda, A. Okamoto, *Photochem. Photobiol. Sci.* **2007**, *6*, 1197.
38 K. L. Taneja, L. M. Lifshitz, F. S. Fay, R. H. Singer, *J. Cell Biol.* **1992**, *119*, 1245.
39 M. V. Matz, A. F. Fradkov, Y. A. Labas, A. P. Savitsky, A. G. Zaraisky, M. L. Markelov, S. A. Lukyanov, *Nat. Biotechnol.* **1999**, *17*, 969.
40 I. L. Hofacker, W. Fontana, P. F. Stadler, L. S. Bonhoeffer, M. Tacker, P. Schuster, *Monatsh. Chem.* **1994**, *125*, 167.